Published in final edited form as:
Cell Rep. 2014 August 7; 8(3): 871–882. doi:10.1016/j.celrep.2014.06.052.

Antigen-specific inhibition of high avidity CTL target lysis by low avidity CTL via trogocytosis: a novel mechanism of immune regulation

Brile Chung[#1], **Tor B. Stuge**[#2,6], **John P. Murad**[1], **Georg Beilhack**[3], **Emily Andersen**[1], **Brian D. Armstrong**[1,6], **Jeffrey S. Weber**[4], and **Peter P. Lee**[1,*]

[1]Department of Cancer Immunotherapeutics & Tumor Immunology (CITI), City of Hope National Medical Center, 1500 E. Duarte Rd, Duarte, CA 91010, USA

[2]Department of Medicine, Division of Hematology, Stanford University, 300 Pasteur Dr., Stanford, CA 94305, USA

[3]Department of Medicine, Division of Bone Marrow Transplantation, Stanford University, 300 Pasteur Dr., Stanford, CA 94305, USA.

[4]Moffitt Cancer Center, University of Southern Florida, 12902 Magnolia Dr, Tampa, FL 33612, USA

[6]Light Microscopy Imaging Core, City of Hope National Medical Center, 1500 E. Duarte Rd, Duarte, CA 91010, USA

[#] These authors contributed equally to this work.

Summary

Current vaccine conditions predominantly elicit low avidity cytotoxic T-lymphocytes (CTLs), which are non-tumor-cytolytic but indistinguishable by tetramer staining or Enzyme-Linked ImmunoSpot from high avidity CTLs. Using CTL clones of high or low avidity for melanoma antigens, we show that low avidity CTLs can inhibit tumor lysis by high avidity CTLs in an antigen-specific manner. This phenomenon operates in vivo: high avidity CTLs control tumor growth in animals, but not in combination with low avidity CTLs specific for the same antigen. The mechanism involves stripping of specific peptide-major histocompatibility complexes (pMHC) via trogocytosis by low avidity melanoma-specific CTLs without degranulation, leading to insufficient levels of specific pMHC on target cell surface to trigger lysis by high avidity CTLs. As such, peptide repertoire on the cell surface is dynamic and continually shaped by interactions

[*]Address correspondence to: Dept. of Cancer Immunotherapeutics & Tumor Immunology (CITI) City of Hope and Beckman Research Institute Beckman Center, room 5109 1500 East Duarte Road, Duarte, CA 91010 Phone: 626.256.4673 x32519 Fax: 626.301.8817 plee@coh.org.
[5]Current address: Immunology Research Group, Department of Medical Biology, University of Tromsø, Hansine Hansens veg 18, 9019 Tromsø, Norway
Current address: Department of Internal Medicine III, Medical University of Vienna, Spitalgasse 23, 1090 Wien, Austria

with T cells. These results describe immune regulation by low avidity T cells and have implications for vaccine design.

Introduction

Cancer vaccines have been shown to elicit detectable CTL responses in patients, but such responses have not correlated with clinical outcome (Lollini et al., 2006). We previously demonstrated that vaccine-elicited T cells are heterogeneous with respect to tumor killing capacity, and only a small subset of vaccine-elicited T cells are efficient at tumor cell lysis (Stuge et al., 2004). This is largely due to differences in functional avidity (also known as recognition efficiency): peptide-specific T cells indistinguishable by tetramer staining may differ by up to 1000-fold in peptide requirement for target lysis. Only high avidity CTLs, which may represent 10% or less of a vaccine-elicited response, could lyse tumor targets (Stuge et al., 2004). Low avidity T cells, which are non-tumor-cytolytic, represent the predominant cell population elicited via vaccine conditions that involve high, supra-physiological antigen doses. Under these conditions, it remains unclear whether low avidity CTLs are simply inert or may actively compete against or interfere with high avidity T cells in tumor lysis.

Prior studies have shown that the competition between antigen-specific T cells for interaction with cognate peptide-MHC complexes plays an important role in determining the levels of immune responses, such as epitope dominance and affinity maturation in secondary T cell responses (Butz and Bevan, 1998; Kedl et al., 2000; Kedl et al., 2002). In these studies, competition occurs at low antigen levels or when there is limited accessibility to surface molecules associated with immunological synapses (i.e. MHC or co-stimulatory molecules) on antigen presenting cells (APCs) during the induction phase (Kedl et al., 2000). In this report, we demonstrate that even after being elicited, anti-tumor activity of high avidity CTL can still be inhibited by low avidity CTL in an antigen-specific manner in vitro and in vivo. This inhibition occurs through a trogocytosis mechanism in which low avidity CTLs strip cognate peptide-MHC complexes from the target cell surface without killing, leaving sub-threshold levels of target peptides accessible to high avidity CTLs. Antigen-specific inhibition of high avidity CTLs by low avidity CTLs represents a novel mechanism of immune regulation.

Results

Low avidity CTL inhibit high avidity CTL mediated tumor cell lysis

We assessed tumor cell lysis by high avidity TAA-specific CTL in the presence or absence of low avidity TAA-specific CTL, or virus-specific CTL as specificity controls. Mel526 cells were pre-incubated with one of three different low avidity HLA-A*02:01-restricted CTL clones specific for the gp100 (209-217) peptide (G209n: ITDQVPFSV) prior to addition of G209n-specific high avidity CTL clones (Figure 1A and 1B). These clones, all isolated from cancer patients, were characterized for efficiency in lysis of mel526 cells and for avidity based on peptide titrations (Table 1). High and low CTL avidity clones were equivalent in lysis of T2 cells pulsed with high levels (1 μg/ml) of cognate peptide, and

hence were all fully competent to kill. Peptide titration curves for a high avidity versus a low avidity clone are shown in Figure S1, demonstrating a 1000-fold difference in peptide responses between these clones that are specific for the same G209 peptide. High and low avidity CTLs differed significantly in their abilities to lyse melanoma targets (Figure 1A and 1C). While the high avidity clone 476.139 efficiently lysed mel526 cells in the absence of low avidity cells (Figure 1A), lysis was inhibited following pre-incubation of the mel526 target cells with each of the low avidity clones (Figure 1B). This inhibition was not merely due to steric hindrance since pre-incubation of mel526 cells with a CTL clone specific for influenza peptide (FLU: GILGFVFTL) resulted in little or no inhibition (Figure 1B). Similar inhibition was seen when assaying for inhibition of mel526 cell lysis by high avidity clones specific for the MART (27-35) peptide (M27: ELAGIGILTV) by pre-incubation of mel526 cells with two low avidity M27-specific clones, but not with a clone specific for CMV peptide (NLVPMVATV) (Figure 1C and 1D). We further confirmed whether target cell death induced by high avidity CTLs is inhibited by the presence of low avidity CTLs via a flow-based apoptosis assay. We found the same inhibitory results in the presence of low avidity CTLs using mel526 target cells. The overall percentage of mel526 cells that were positive for both 7AAD and Annexin V was significantly less in the presence of low avidity CTLs at 4 and 24 hour time points (Figure 1E) (4 hour time point; High vs. Low; $p \leq 0.01$, High vs. Low + High; $p \leq 0.016$; 24 hour time point; High vs. Low; $p \leq 0.01$, High vs. Low + High; $p \leq 0.01$). Inhibition by low avidity CTL clones of target lysis was also found with MeWo cells, and additionally, the optimal inhibition time was determined to be after one hour pre-incubation of melanoma cells with low avidity CTL (Figure S2). Thus, the presence of low avidity CTL clones inhibits lysis of melanoma cells by high avidity CTL.

High avidity CTL lysis of tumor cells *in vitro* and control of tumor growth *in vivo* is inhibited by low avidity CTLs in an antigen-specific manner

To determine if this inhibitory effect is antigen-specific, mel526 cells were incubated with low and high avidity CTL clones specific for G209n, MART, or viral peptides in various combinations (Figure 2A and 2B). Maximal inhibition was detected only when low and high avidity clones of the same peptide specificity were combined with melanoma targets. While high avidity G209n-specific CTLs were significantly inhibited by low avidity G209n-specific CTLs, low avidity MART-specific CTLs had little to no inhibition, similar to that of viral antigen-specific CTLs (Figure 2A). An identical pattern was seen with high avidity MART-specific CTLs and low avidity MART-specific CTLs, but not G209n- specific CTLs (Figure 2B). Inhibition was antigen-specific since high avidity and low avidity CTLs specific for two different antigens (MART or G209n) did not significantly cross-inhibit. This pattern was confirmed using a number of different low avidity G209n- specific and MART-specific clones (Figure S3). The antigen-specific nature of inhibition suggests that low avidity CTLs prevent high avidity CTLs from recognizing or responding to specific peptide-MHC complexes on the surface of target cells.

To examine whether inhibition of high avidity CTL lysis of tumor cells by low avidity CTL could occur in vivo, we injected SCID mice with melanoma cells subcutaneously followed by intravenous injections of various combinations of high avidity CTLs with low avidity or virus-specific CTLs. Tumor size was monitored to 40 days after CTL injections. In mice

injected with a combination of high avidity and low avidity G209n-specific CTLs, tumor growth was significantly higher than in mice injected with high avidity G209n-specific CTLs alone ($p<0.01$), or high avidity G209n-specific CTLs together with FLU-specific CTLs ($p=0.02$) (Figure 2C). These results demonstrate that this antigen-specific CTL inhibition can also take place in vivo.

Tetramer decay reveals low avidity CTLs have lower relative TCR affinity for native peptide as compared to high avidity CTLs

T cell avidity is driven primarily by TCR affinity for its cognate peptide (Corse et al., 2011; Denton et al., 2011; Gourley et al., 2004), and also expression levels of CD3/TCR complex and adhesion molecules. We determined that high and low avidity clones expressed CD3/TCR at similar levels (data not shown). To assess relative TCR affinities of the high and low avidity CTLs, we utilized the tetramer decay assay which has been validated to determine the relative TCR affinity of intact T cells (Savage et al., 1999; Turner et al., 2008; Wang and Altman, 2003). Low avidity G209-specific CTL clone showed significantly more rapid tetramer decay kinetics ($p<0.01$) than the high avidity clone. Results plotted show the reduction in tetramer MFI, normalized to initial MFI at 0 minutes, which represent the tetramer decay in low avidity CTLs (○) and high avidity CTLs (□) over time (Figure 2D). These results strongly support that TCR affinity for the native peptide is higher for the high avidity clone than the low avidity clone.

Visualizing CTL cross-inhibition in three dimensional (3D) culture system

To model and study the in vivo situation, we generated a three-dimensional culture system to replicate *in vivo* tumor-T cell interactions. Cell aggregates were formed by centrifugation of G209n-specific CTLs with mel526 cells and culturing these aggregates on nucleopore filters (Figure 3A). Based on immunohistochemical analyses, mel526 aggregates mixed with either low avidity CTLs only or the combination of both high and low CTLs led to much lower numbers of mel526 cells expressing apoptotic marker caspase 3 as compared to aggregates containing mel526 and only high avidity CTLs (Figure 3B). As shown in Figure 3C, counts of viable (non-lysed) mel526 cells in a fixed dimension area for each slide was identified by utilizing Image Pro Premier automated cell counting for each tumor/CTL aggregate combination. The results indicate a statistically significant reduction in the number of viable mel526 cells in the presence of high avidity CTLs only as compared low avidity CTLs ($p<0.0001$) or the combination of both low and high avidity CTLs ($p<0.0001$). In addition, similar results were also observed when mel526 3D spheroids were challenged with the different combination of high and low avidity CTLs (Figure S4). Because tumor spheroids resemble many similar aspects of tumor microenvironments, they are commonly utilized to study the efficacy of anti-tumor treatments (Zhang et al., 2005). When the emission of fluorescence signals from calcein labeled mel526 cell spheroids in the presence of G209n-specific CTLs were evaluated, we detected the significantly reduced levels of fluorescence in the presence of high avidity CTLs compared to low or high plus low avidity CTLs. These analyses demonstrate that, in addition to the higher tumor specific lytic capacity of the high avidity CTLs in comparison to low avidity CTLs against mel526, low avidity CTLs can inhibit tumor lysis by high avidity CTLs in the 3D tumor spheroid and

aggregate co-culture models. Error bars represent standard deviation between assays (High vs. Low; $p \leq 0.01$, High vs. Low + High; $p \leq 0.01$).

Low avidity CTLs strip specific peptide-MHC complexes from the surface of target cells

We hypothesized that interaction of low avidity CTLs with target cells may lead to modulation of the target cell's surface antigens without cytolysis. To test this hypothesis, target cells were incubated with G209n peptides containing a biotinylated linker peptide. Biotin/peptide-pulsed target cells were then incubated with low avidity G209n-specific or viral antigen-specific CTL clones, then reacted with streptavidin-PE and analyzed by flow cytometry to determine the potential down-modulation of specific peptide-MHC complexes on the surface of target cells following interaction with CTL. Indeed, target cells incubated with low avidity G209n-specific CTL clones bound less streptavidin-PE compared to target cells treated with FLU- specific CTL or no CTL, suggesting that the target cell surface density of G209n peptide-MHC complexes had been reduced by interaction with low avidity G209n-specific CTLs (Figure 4A).

We reasoned that a potential mechanism of inhibition could be stripping of specific peptide-MHC complexes on the target cell surface by low avidity TAA-specific T cells via trogocytosis or other forms of sequestration (Hudrisier et al., 2005; Tomaru et al., 2003; Uzana et al., 2012). To test this hypothesis, we used immortalized B-cells expressing HLA-A*02:01 coupled to GFP (HmyA2GFP cells) pulsed with G209n peptide, and incubated them with G209n-specific low avidity CTLs (Tomaru et al., 2003). Within 15 minutes, formation of conjugates between CTLs and HmyA2GFP cells were visualized, and small membrane fragments of HLA-GFP expression on the surface of CD8+ T cells appeared after 30 minutes (Figure 4B and Supplemental video 1). Based on previous reports indicating that the specificity of peptide-HLA-TCR recognition initiates trogocytosis, and that consistent TCR stimulation results in elevated intracellular calcium concentration in T cells, we examined the fluctuation of intracellular calcium levels in both high and low avidity CTLs during trogocytosis (Joseph et al., 2013; Osborne and Wetzel, 2012). As shown in Figure 4C, an increase in intracellular calcium concentration is directly associated with both high and low avidity CTLs undergoing trogocytosis, indicating that TCR signaling precedes trogocytosis. We next postulated that the level of trogocytosis is directly associated with the amount of peptides presented. Different concentrations of G209n peptide were pulsed onto HmyA2GFP cells and incubated with either high or low avidity G209n specific CTLs. The percentage of GFP+ CTLs following incubation revealed that the capacity for trogocytosis of both high and low avidity G209n clones directly correlated to the amount of G209n peptide concentration. Importantly, low avidity CTLs displayed a similar trogocytosis capacity as compared with high avidity CTLs, further reflecting their ability to reduce specific peptide-MHC complexes on the surface of target cells (Figure 5A).

We then examined whether or not tumor cells could induce trogocytosis by G209n-specifc CTLs. To test this, we used PKH67 labeled mel526 as the target. As shown in Figure 5B, the level of fluorescence signals detected from both high and low avidity G209n specific CTLs was not significantly different (12.6% from High vs. 13.1%. from Low). This result fits within the range of earlier G209 peptide dependent trogocytosis in Figure 5A (concentration

of G209n peptide between 1pg and 0.1pg/ml). Taken together, these results show that low avidity CTL can strip peptide-MHC complexes from target cells via trogocytosis even at peptide concentrations that are too low to induce target cell killing by these cells.

Degranulation following trogocytosis in high vs. low avidity CTL

Given that both high and low avidity G209n-specific CTL clones displayed similar capacity for trogocytosis following interaction with G209n peptide-pulsed HmyA2GFP cells, we wanted to examine to what extent trogocytosis by low avidity CTL can reduce the cytolytic ability of high avidity CTL. To accomplish this we measured mobilization of CD107 (LAMP-1), a surrogate marker for lysosomal degranulation, on CTLs in relation to trogocytosis (Rubio et al., 2003). HmyA2GFP cells were pulsed with G209n peptides, incubated with either high or low avidity CTLs, and analyzed for the expression of CD107 on GFP-positive CTLs (Red boxes, Figure 6A). The level of GFP in both high and low avidity CTLs was similar, suggesting that their ability to trogocytose in a dose-dependent fashion is relatively similar. The majority of high avidity CTLs expressing CD107 were also positive for GFP, supporting a strong correlation between trogocytosis and degranulation activity. In contrast, we observed that the percentage of CD107 from GFP-positive low avidity CTLs was significantly less than that of high avidity CTL. Similar results were observed with PKH67-labeled mel526 cells as a target; a considerably higher frequency of PKH67-positive CTLs (Red boxes, Figure 6B) was observed with high avidity CTLs (29.1%) compared to low avidity CTLs (6.9%). Moreover, the frequency of CD107 expression specifically in pre-stained and positively gated high avidity CTLs was reduced by 50% (down to 15.8% from 29.1%) when the mel526 cells were pre-incubated with low avidity G209n-specific CTL clones. The inhibitory effects of low avidity CTLs at different ratios on CD107 expression by high avidity CTLs are shown in Figure 6C. In all, these data demonstrate that low avidity CTLs can inhibit degranulation of high avidity CTLs against tumor cells.

Discussion

It is increasingly recognized that antigen recognition by T cells is not Boolean but depends on avidity and the availability of cognate peptides on the target cell surface. Our results reveal another level of complexity in T cell recognition by demonstrating that low avidity CTLs can inhibit target lysis by high avidity CTLs in an antigen-specific manner. The mechanism of inhibition involves stripping of specific pMHC complexes by low avidity CTLs without cytolysis via trogocytosis, thus transiently reducing the availability of cognate pMHC complexes on the target cell surface for interaction with high avidity CTLs. As such, CTLs may constantly modulate the repertoire of pMHC complexes on target cells, even in the absence of a cytolytic response, via low-affinity TCR-pMHC interactions.

Competition for antigen and peptide MHC complexes is a known phenomenon and is thought to shape the repertoire of cells responding to a limited amount of antigen (Kedl et al., 2003; Kedl et al., 2000; Kedl et al., 2002). The outcome is the selection of lymphocytes with the highest affinity for antigen and suppression of lymphocytes with lower affinity receptors. This occurs during the induction phase under low antigen abundance. We

previously demonstrated that antigen-specific CTLs elicited via peptide vaccines in melanoma patients are predominantly low avidity and poor at tumor lysis, with relatively few high avidity CTLs that lysed tumor cells efficiently (Stuge et al., 2004). This may seem paradoxical in light of the prior studies of competition for antigen, but the key difference is antigen availability. Current vaccine approaches generally involve high antigen doses, which favor expansion of low avidity CTLs as these are more abundant than high avidity specific CTLs due to cross-reactivity. In contrast, competition for antigen and selection of dominant high avidity clones has been observed only when antigen is at limited densities (Kedl et al., 2003; Kedl et al., 2000; Kedl et al., 2002).

In this study, we demonstrated using fluorescent microscopy that both high and low avidity CTLs can effectively capture cognate peptide-MHC complexes from target cells via trogocytosis. We further demonstrated that biotin/peptide-pulsed mel526 target cells incubated with low avidity G209n-specific CTL clones displayed less streptavidin-PE expression, confirming that the surface density of G209n peptide-MHC complexes had been reduced by interaction with low avidity G209n-specific CTLs. Importantly, low avidity CTLs displayed similar capacity to undergo trogocytosis as that of high avidity CTLs but with little to no degranulation or cytotoxicity. Low avidity CTLs were fully competent to lyse target cells presenting cognate peptide at higher concentrations (Figure S1), confirming that these cells were functionally cytolytic. We further investigated whether increasing the availability of cognate peptides on target cells reduced the inhibitory effect by low avidity CTLs. Indeed, increasing the concentration of G209n peptide resulted in a reduction of the inhibitory effect by low avidity CTLs (Figure S6), further confirming that the antigen-specific inhibitory effect is dependent on peptide availability on the target cell surface.

The Jacobson and Lotem groups demonstrated that trogocytosis could be used to detect and isolate antigen-specific CTLs via either transfer of pMHC complexes (Tomaru et al., 2003), membrane (Machlenkin et al., 2008), or surface antigens (Eisenberg et al., 2013). Using trogocytosis and signaling analysis, the Lotem group also demonstrated that a peptide-specific (MART26-35) TIL response consisted of individual T cells with different functional responses (Uzana et al., 2012), consistent with our previous findings that only high avidity TAA-specific T cells could kill tumor cells (Stuge et al., 2004). An important distinction between the work presented here and these prior publications is our focus on the interplay between T cells of different avidities for the same antigen, and between T cells specific for different antigens (MART and gp100). Our use of HLA-A2-GFP transfer from target to T cells to measure trogocytosis provided a very sensitive and specific readout, allowing us to detect trogocytosis down to the picogram level of specific peptides. This allowed us to demonstrate that T cells have different peptide thresholds for trogocytosis versus cytotoxicity (Figure S6). Differences in downstream signaling properties of high and low avidity CTLs that underlie their different functional responses are currently under investigation.

These findings have clinical implications. The inhibitory effect of low avidity CTLs on high avidity CTL tumor lysis could at least in part explain the poor clinical responses observed in many cancer peptide vaccine trials (Rosenberg et al., 2004). As such, vaccines targeting T cell responses need to take into account avidity. This applies not only to cancer vaccines, but

also vaccines for infectious diseases. These findings also have implications in self-tolerance. It is well established that low avidity CTLs specific for self peptides exist in the mature T cell repertoire (Bouneaud et al., 2000; de Visser et al., 2000; Redmond and Sherman, 2005). These cells could inhibit occasional high avidity CTLs specific for self antigens that may escape negative selection. As such, antigen-specific inhibition of high avidity CTL by low avidity CTL represents a novel form of immune regulation.

Experimental Procedures

Cells

HLA-A*0201-restricted clonal G209n-specific (gp100: 209–217 [ITDQVPFSV]) and M27-specific (MART: 26–35 [ELAGIGILTV]) CD8-positive T cells lines are listed in Table 1 and have been characterized previously (Stuge et al., 2004). CMV-specific (CMVpp65: 495-503 [NLVPMVATV]) and FLU-specific (Influenza A virus M1: 58-66 [GILGFVFTL]) CTL clones were generated from healthy donor peripheral blood mononuclear cells as previously described (Stuge et al., 2004). All clones were maintained by bi-weekly stimulation with anti-CD3 and irradiated feeder cells. Cells were used in assays between day 15 and 21 following stimulation. Melanoma cells and T2 cells were maintained in cell culture medium (Iscove's Modified Dulbecco's Medium [IMDM] and 10% FBS) while CTL clones were maintained in "CTL medium" (cell culture medium supplemented with 2% human AB serum). The HLA-A*0201-positive melanoma line (mel526) was obtained from the Surgery Branch of the NCI. The HLAA*0201-positive melanoma line (MeWo) and the T2 cell line were purchased from ATCC (Manassas, Virginia, United States) and maintained according to instructions provided by ATCC. Mel526 and MeWo express both MART and gp100 as confirmed by immunohistochemical staining. Cells were trypsinized using Trypsin/EDTA solution (GIBCO, San Diego, California, United States) before use. T2 cells are HLA-A*0201- positive and were pulsed prior to assays with peptides indicated in the text below. The immortalized B-cell line expressing HLA-A*201 coupled to GFP (HmyA2GFP cells) was obtained from NIH (generous gift of Dr. Steven Jacobson) (Tomaru et al., 2003). To generate HmyA2GFP cells, the HLA-A and B locus defective B-cell line (Hmy2.CIR) was transfected with the RSV-HLA-A2 vector containing GFP expression.

Cytotoxic Assays

Cytotoxic assays were performed using the 51-Chromium (^{51}Cr)-release assay as described previously (Stuge et al., 2004). Briefly, mel526, MeWo, or T2 cells were labeled overnight with ^{51}Cr, and then washed and suspended to 10^5 cells/ml. One hundred microliters of target cells were incubated with 100 μl CTL clones at various effector-to-target (E:T) ratios in round bottom 96-well tissue culture plates and centrifuged 200xg for 1 minute to bring together the cells at the bottom of the plate and initiate the assay. Following a 4 hour incubation at 37°C and 7.0% CO_2 cells were resuspended with a multi-channel pipette, centrifuged 550xg for 5 minutes. Forty microliters of cell-free supernatantwas transferred from each well to 60 μl scintillation fluid, mixed well and counts per minute (cpm) were determined by scintillation counting. Percent specific release (PSR) of ^{51}Cr from target cells was calculated by the formula: 100 × [cpm (experimental) - cpm (minimum release)] / [cpm (maximum release) - cpm (minimum release)]. Maximum release wells received 100 μl 2%

Nonidet P-40 (Sigma, St. Louis, MO) instead of CTLs to lyse all target cells. Minimum release wells received 100 μl CTL medium instead of CTLs. Inhibition of tumor lysis by low avidity CTL was assessed as follows unless indicated otherwise: one hundred microliters of ^{51}Cr-labeled target cells were incubated with 50 μl low avidity TAA-specific CTL clones, or viral antigen-specific CTL clones, at various E:T ratios for 1 or 1.5 hours. PSR of ^{51}Chromium from target cells was calculated from 40 μl cell-free supernatants as described above. Percent inhibition was calculated by the formula: 100 × [PSR(high avidity + target) − PSR(low + high avidity + target)]/ PSR(high avidity + target). All assays were performed in triplicate.

Tetramer decay assay to elucidate differences in T cell avidity

The rate of dissociation of bound pMHC tetramers from antigen-specific T cells upon addition of a competing antibody or Fab fragment may be used as a relative measure of the difference in TCR affinities between T cells (Savage et al., 1999). The method we employed utilized iTag™ MHC Class I Human Tetarmer –SA-PE (MBL International Corp, Woburn MA). Tetramer at 5μg/ml and 1:200 dilution of fitc primary conjugated anti-CD8 (clone 3B5, BD Biosciences) was incubated with 0.5×10^6 low and high avidity cells individually at room temperature for 30 minutes. Cells were washed 3 times with ice cold PBS and kept at 4° C for the duration of the assay. Fab fragment of blocking antibody, HLA-A2 antibody (GeneTex, Irvine CA), was generated by using Pierce Fab Micro Preparation Kit (Thermo Scientific, Rockford IL). To the tetramer/CD8 stained high and low avidity CTLs, 20 μM of fab fragment HLA-A2 was added to block tetramers from re-binding once dissociated. Control cells were stained with tetramer and CD8 but without HLA-A2 fab fragment blocking. Aliquots of the high and low populations were collected and re-suspended in 2% paraformaldehyde at time points 0, 10, 20, 30, 50, and 75 minutes. Samples were analyzed by FACS FlowJo software (Treestar, San Carlos CA) to determine decay of fluorescent intensity of tetramer positive cells gated CD8 population over time. Analysis was performed on data collected from three separate experiments. Data were fitted using a linear mixed effects model to test intercept and slope over time by group effects. Calculations were based on the nlme package in R version 2.12.1.

Peptides and peptide pulsing

T2 cells, mel526, or HmyA2GFP cells were pulsed with the HLA-A*02:01 binding gp100(209-217) (ITDQVPFSV) peptide or an extended variant connected to a flexible 17 amino acid linker peptide with a biotinylated C terminus: ITDQVPFSV-GGGSGGGSGGGSGGGSK-biotin (G209n-linker-biotin). Cells were pulsed 1 hour with indicated peptide concentrations at 37°C in 7.0% CO_2 in 3 ml culture medium. Pulsed cells were washed 3x with 10 ml RPMI-1640 with 5% normal calf serum (NCS) and suspended in CTL medium. To monitor modulation of antigenic peptide on target cell surfaces, 10^5 T2 cells pulsed with 10 μM biotinylated G209n-linker-biotin were incubated with or without 10^6 low avidity G209n-specific or FLU-specific CTL clones in 200 μl CTL medium in a 96-well round bottom tissue culture plate containing 1.0 μl anti-CD107a and 0.5 μl anti-CD107b mAbs conjugated with APC (to simultaneously monitor degranulation by CTL) at 37°C in 7.0% CO_2. After 90 minutes cells were transferred to 5 ml FACS tubes (Becton Dickinson). Cells were then washed and suspended in 100 μl CTL medium with 1:100

dilutions of FITC conjugated anti-human CD8 and streptavidin-PE (Caltag) and incubated 30 minutes on ice. Cells were washed, resuspended in PBS 5% NCS, and analyzed by flow cytometry.

Measurement of calcium flux

High and low avidity G209n peptide specific CTLs were suspended in 1 ml of RPMI 1640 media (Life Technologies) supplemented with 10% FBS and 1% PenStrep (Life Technologies) to a final count of 1.0×10^6 cells/ml and cells were centrifuged and re-suspended in 1 ml of 1x PBS in a 1.7ml centrifuge tube. A Rhod-3AM cell permanent fluorescent calcium indicator kit (Life Technologies) was used to determine small changes in intracellular calcium concentrations in stimulated low and high avidity CTLs by FACS analysis. CTLs were loaded with a final concentration of 0.75 μM Rhod-3AM along with 1:250 dilution of APC conjugated anti-human CD8a antibody HIT8a clone (Biolegend) to isolate CD8-positive CTLs. Cells were incubated at 37°C for 45 minutes in the dark, pelleted, and then washed two times with 1x PBS to remove residual Rhod-3AM stain. Cells were stimulated with HmyA2GFP APCs and were previously pulsed with (G209n) peptide at a concentration of 100 pg/ml. APCs were coated on round bottom 96-well plates prior to addition of CTLs. Plate was flash spun for 30 seconds to encourage cell-cell interactions and timer of stimulation was started. Stimulation was performed at a ratio of 1 APC for every 3 CTLs. After 7 minutes of stimulation, cells were transferred to a FACS tube and run on FACSCalibur (BD Biosciences) for FACS analysis. Cells were gated to isolate for CD8-positive CTLs, and GFP expression on CD8-positive cells was utilized as a positive indicator of acquisition of MHC-peptide complexes via trogocytosis. CD8 CTLs were analyzed for differences in calcium fluorescence between trogocytosis (GFP) positive and negative CTLs.

Fluorescent cell membrane labeling

To achieve a GFP-like expressing cellular membrane on mel526 cells for imaging and FACS analysis purposes, a PKH67 fluorescent cell linker dye kit (Sigma-Aldrich) was utilized. mel526 cells were resuspended in 1x PBS at a final count of $1.0\text{-}2.0\times10^6$ cells/ml. Cells were spun down at 1000rpm for 5 minutes and all supernatant was removed and cells resuspended in 500 μl Diluent C. In a separate 1.7ml centrifuge tube PKH67 dye was prepared to a working concentration of 1 μM in 500μl of Diluent C. The 1μM PKH67 dye was mixed with 500μl cell suspension into a 2 ml centrifuge tube resulting in 0.5 μM PKH67 dye final concentration. Cells were allowed to incubate for 5 minutes at 37°C in the dark. Cells were washed with 800μl FBS to stop staining reaction, spun to a pellet at 1000rpm for 10 minutes, and subsequently washed with 2 ml 1x PBS two times to remove excess stain. Cells were resuspended in 1ml of 1x PBS and ready for use and analysis.

Live cell imaging

Live cell analysis was performed to visualize the exchange of membrane proteins via trogocytosis in interactions between CD8+ low and high avidity G209n-specific CTLs and GFP expressing HmyA2GFP APCs pulsed with G209n peptide. To perform these experiments we utilized a Zeiss Axio Observer Z1 Inverted Microscope coupled to an Exfo Xcite fluorescence illumination apparatus capable of detecting DAPI, eGFP, DS Red, and

Far Red emission spectra. Images were captured via a Hamamatsu EMCCD C9100-13 Monochrome Camera and Zeiss MRc5 Digital Color Camera. A 63X/1.3NA Plan-NeoFluar Multi Immersion objective was coupled with Optovar 1.6X magnification resulting in 100X final magnification. Live cell imaging was aided by a Pecon/Zeiss incubation system with heated stage insert and enclosure with 5% CO_2 control. Cells were placed on 35mm poly-d-lysine coated glass bottom dishes (MatTek Corporation, P35GC-1.5-10-C). All analysis was performed using Zeiss AxioVision software version 4.8 for Microsoft Windows.

Generation of tumor aggregates

To generate a mel526 tumor/CTL aggregate, approximately 2×10^5 mel526 plus 1×10^5 high or low avidity CTLs mel526 were mixed together in PBS (Mediatech, Inc, Manassas, VA) and spun into an aggregate pellet in a microcentrifuge tube. Following removal of the supernatant, the aggregate was drawn into a micropipette tip (no more than 10μl in volume) and released onto the surface of a nucleopore filter membrane (0.8 μm pores; Millipore, Billerica, MA) floating on gelfoam (Pharmacia & Upjohn, Bridgewater, NJ) in D10 medium. The tumor/CTL aggregate was then harvested after 48 hours in culture for analysis of apoptosis.

Quantification of viable mel526 cells in tumor/CTL aggregate

In attempts to identify the cytolytic consequences of high avidity CTLs versus low avidity CTLs in our mel526 tumor aggregate model, we adopted a viable cell counting methodology. The aggregate pellet described above was formalin fixed and paraffin embedded and sliced to 3μm and placed on glass slides for imaging purposes. The segments then underwent immunohistochemical staining for melan A (DAB: brown), caspase 3 (fast red), and hematoxylin (blue). Images of slide segments were taken at 20x magnification and identical large regions of interest of the aggregate were cropped at a fixed dimension for all slide images. Images were analyzed with Image Pro Premier 9.0 for Windows utilizing an automated cell counting feature. A selection of intact cells within the region of interest was manually selected to establish criteria for non-lysed cells. The software then identified counts of the cells that met the criteria within the fixed dimension region of interest for each tumor/CTL aggregate slide. Quantification of viable non-lysed cells were collected for 6 regions of interest for each mel526 aggregate with either high avidity CTLs, low avidity CTLs, or a combination of low and high avidity CTLs. Statistical analysis was performed using an unpaired t-test of groups counts with significance assigned with $p<0.05$.

In vivo experiments

C57BL/6J x C57BL/10SgSnAi)-[KO]γc-[KO]Rag2 mice were purchased from Taconic Farms. For in vivo assessment of tumor growth in the presence of T cell clones, mice were injected subcutaneously in the left flank with 1.0×10^6 mel526 cells in 50 μl PBS. To facilitate injections and measurements, the fur was shaved from left flank before injection of tumor cells and before determination of subcutaneous tumor size. One day after tumor cell injection, the mice were injected intravenous (i.v.) or retro-orbital (r.o.) with 5.0×10^6 gp100-specific high avidity CTL (in 50 μl PBS) (tu hi), gp100-specific high avidity CTL combined with 3.0×10^7 gp100-specific low avidity CTL (in 100 μl PBS) (tu hi lo), or gp100-specific high avidity CTL combined with 3.0×10^7 flu-specific CTL (tu hi flu). After 40 days, tumor

volume was estimated in each mouse: subcutaneous tumor length (longest diameter) and width was estimated externally using a caliper and the volume was calculated by the formula Tumor volume = 1/2(length × width^2) All mice were euthanized after tumor volume measurement on day 40.

CD107 Mobilization Assay

High and low avidity CTL, mel526 (pulsed or non-pulsed), peptide-pulsed T2, or HmyA2GFP (pulsed or non-pulsed) cells were combined as described in figure legends for the individual experiments. Assays were performed as described previously (Rubio V et al., 2003; Betts MR et al., 2003). Briefly, the following was added in order to each well: 1 μl of 2 mM monensin (Sigma, St. Louis, Missouri, United States) in 100% EtOH, 100 μl of target cells, 100 μl of effector cells, and 1 μl anti-CD107a and 0.5 μl anti-CD107b mAbs conjugated to allophycocyanin (APC). For the inhibition assays, target cells were preincubated with 50 μl low avidity CTL for 1.5 hours prior adding 50 μl high avidity CTL. E:T ratios were as indicated for the individual experiments. The cells were mixed using a multichannel pipette at each addition of cells. The plate was centrifuged at 200*g* for 1 minute to pellet cells, then incubated at 37°C, 7.0% CO_2 for the indicated time periods. After the incubations, the plates were centrifuged to 500*g* to pellet cells, and the supernatant was removed. Cell–cell conjugates were disrupted by washing the cells with PBS supplemented with 0.02% azide and 0.5 mM EDTA, and mixed vigorously, then stained with Phycoerythrin (PE) conjugated anti-human CD8 antibodies (Caltag Laboratories, Burlingame, California, United States) and analyzed by flow cytometry using a two-laser, four-color FACSCalibur. CTL were identified by forward and side scatter signals, and then selected for CD8-positive cells.

Supplementary Material

Refer to Web version on PubMed Central for supplementary material.

Acknowledgments

We thank Dr. Steve Jacobsen (NIH) for kindly providing the HLA-A2-GFP cells, and Alexandre Johannsen for technical assistance. This work was supported by a DoD BCRP Era of Hope Expansion Award (to PPL). Research reported in this publication included work performed in the Analytical Cytometry Core supported by the National Cancer Institute of the National Institutes of Health under award number P30CA33572. The content is solely the responsibility of the authors and does not necessarily represent the official views of the National Institutes of Health.

References

Bouneaud C, Kourilsky P, Bousso P. Impact of negative selection on the T cell repertoire reactive to a self-peptide: a large fraction of T cell clones escapes clonal deletion. Immunity. 2000; 13:829–840. [PubMed: 11163198]

Butz EA, Bevan MJ. Massive expansion of antigen-specific CD8+ T cells during an acute virus infection. Immunity. 1998; 8:167–175. [PubMed: 9491998]

Corse E, Gottschalk RA, Allison JP. Strength of TCR-peptide/MHC interactions and in vivo T cell responses. Journal of immunology (Baltimore, Md : 1950). 2011; 186:5039–5045.

de Visser KE, Cordaro TA, Kioussis D, Haanen JB, Schumacher TN, Kruisbeek AM. Tracing and characterization of the low-avidity self-specific T cell repertoire. European journal of immunology. 2000; 30:1458–1468. [PubMed: 10820394]

Denton AE, Wesselingh R, Gras S, Guillonneau C, Olson MR, Mintern JD, Zeng W, Jackson DC, Rossjohn J, Hodgkin PD, et al. Affinity thresholds for naive CD8+ CTL activation by peptides and engineered influenza A viruses. Journal of immunology (Baltimore, Md : 1950). 2011; 187:5733–5744.

Eisenberg G, Uzana R, Pato A, Frankenburg S, Merims S, Yefenof E, Ferrone S, Peretz T, Machlenkin A, Lotem M. Imprinting of lymphocytes with melanoma antigens acquired by trogocytosis facilitates identification of tumor-reactive T cells. Journal of immunology (Baltimore, Md : 1950). 2013; 190:5856–5865.

Gourley TS, Wherry EJ, Masopust D, Ahmed R. Generation and maintenance of immunological memory. Seminars in immunology. 2004; 16:323–333. [PubMed: 15528077]

Hudrisier D, Riond J, Garidou L, Duthoit C, Joly E. T cell activation correlates with an increased proportion of antigen among the materials acquired from target cells. European journal of immunology. 2005; 35:2284–2294. [PubMed: 16021601]

Joseph N, Reicher B, Barda-Saad M. The calcium feedback loop and T cell activation: How cytoskeleton networks control intracellular calcium flux. Biochimica et biophysica acta. 2013

Kedl RM, Kappler JW, Marrack P. Epitope dominance, competition and T cell affinity maturation. Current opinion in immunology. 2003; 15:120–127. [PubMed: 12495743]

Kedl RM, Rees WA, Hildeman DA, Schaefer B, Mitchell T, Kappler J, Marrack P. T cells compete for access to antigen-bearing antigen-presenting cells. The Journal of experimental medicine. 2000; 192:1105–1113. [PubMed: 11034600]

Kedl RM, Schaefer BC, Kappler JW, Marrack P. T cells down-modulate peptide-MHC complexes on APCs in vivo. Nature immunology. 2002; 3:27–32. [PubMed: 11731800]

Lollini PL, Cavallo F, Nanni P, Forni G. Vaccines for tumour prevention. Nature reviews Cancer. 2006; 6:204–216.

Machlenkin A, Uzana R, Frankenburg S, Eisenberg G, Eisenbach L, Pitcovski J, Gorodetsky R, Nissan A, Peretz T, Lotem M. Capture of tumor cell membranes by trogocytosis facilitates detection and isolation of tumor-specific functional CTLs. Cancer research. 2008; 68:2006–2013. [PubMed: 18339883]

Osborne DG, Wetzel SA. Trogocytosis results in sustained intracellular signaling in CD4(+) T cells. Journal of immunology (Baltimore, Md : 1950). 2012; 189:4728–4739.

Redmond WL, Sherman LA. Peripheral tolerance of CD8 T lymphocytes. Immunity. 2005; 22:275–284. [PubMed: 15780985]

Rosenberg SA, Yang JC, Restifo NP. Cancer immunotherapy: moving beyond current vaccines. Nature medicine. 2004; 10:909–915.

Rubio V, Stuge TB, Singh N, Betts MR, Weber JS, Roederer M, Lee PP. Ex vivo identification, isolation and analysis of tumor-cytolytic T cells. Nature medicine. 2003; 9:1377–1382.

Savage PA, Boniface JJ, Davis MM. A kinetic basis for T cell receptor repertoire selection during an immune response. Immunity. 1999; 10:485–492. [PubMed: 10229191]

Stuge TB, Holmes SP, Saharan S, Tuettenberg A, Roederer M, Weber JS, Lee PP. Diversity and recognition efficiency of T cell responses to cancer. PLoS medicine. 2004; 1:e28. [PubMed: 15578105]

Tomaru U, Yamano Y, Nagai M, Maric D, Kaumaya PT, Biddison W, Jacobson S. Detection of virus-specific T cells and CD8+ T-cell epitopes by acquisition of peptide-HLA-GFP complexes: analysis of T-cell phenotype and function in chronic viral infections. Nature medicine. 2003; 9:469–476.

Turner MJ, Jellison ER, Lingenheld EG, Puddington L, Lefrancois L. Avidity maturation of memory CD8 T cells is limited by self-antigen expression. The Journal of experimental medicine. 2008; 205:1859–1868. [PubMed: 18625745]

Uzana R, Eisenberg G, Sagi Y, Frankenburg S, Merims S, Amariglio N, Yefenof E, Peretz T, Machlenkin A, Lotem M. Trogocytosis is a gateway to characterize functional diversity in melanoma-specific CD8+ T cell clones. Journal of immunology (Baltimore, Md : 1950). 2012; 188:632–640.

Wang XL, Altman JD. Caveats in the design of MHC class I tetramer/antigen-specific T lymphocytes dissociation assays. Journal of immunological methods. 2003; 280:25–35. [PubMed: 12972185]

Zhang X, Wang W, Yu W, Xie Y, Zhang X, Zhang Y, Ma X. Development of an in vitro multicellular tumor spheroid model using microencapsulation and its application in anticancer drug screening and testing. Biotechnology progress. 2005; 21:1289–1296. [PubMed: 16080713]

Highlights

- Low avidity CTL inhibit high avidity CTL target lysis in an antigen-specific manner
- Low avidity CTL strip specific pMHC complexes from target cells without lysis
- Peptide repertoire on the cell surface is dynamic and shaped by interactions with T cells
- Design of T cell vaccines needs to account for avidity

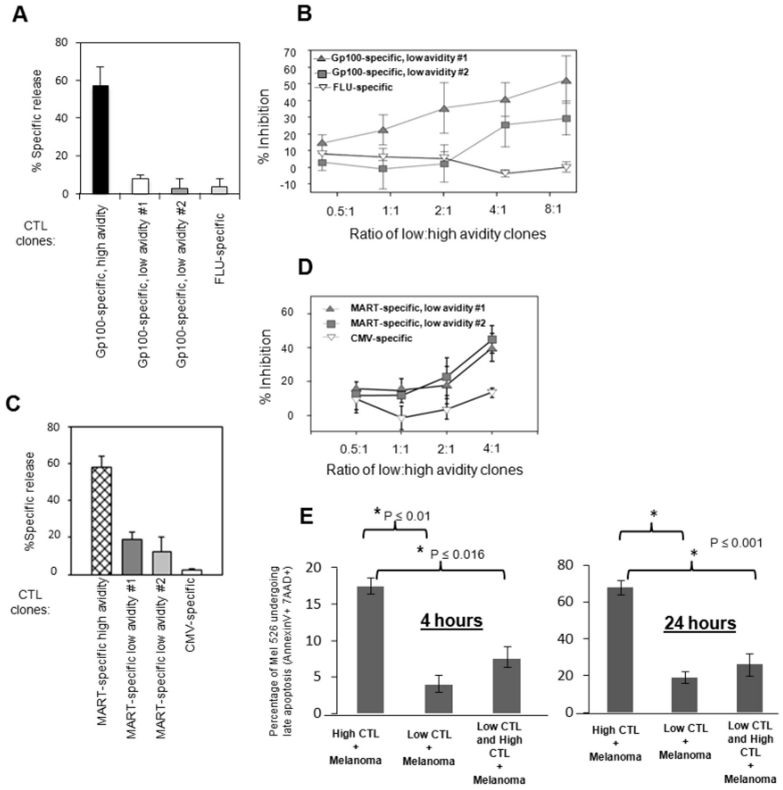

Figure 1. TAA-specific low avidity CTL can inhibit lysis of melanoma cells by high avidity CTL.

(A) and **(B)**: Gp100-specific CTL clones. C and D: MART-specific CTL clones. (**A**) and (**C**): High and low avidity CTL clones vary greatly in efficiency at tumor cell lysis, (**B**) and (**D**): High avidity CTL lysis of tumor cells can be inhibited by pre-incubation of tumor cells with non-tumor lytic low avidity CTL. For each assay in B and D, 10^4 51-Chromium(Cr)-labeled mel526 melanoma cells were combined with 5×10^4 to 8×10^5 low avidity TAA-specific or virus antigen- specific CTL by centrifugation at 200xg and incubated 1.5 hours before addition of 10^5 high avidity TAA-specific CTL to a final volume of 200 μl. This was followed by additional 1.5 hour incubation. For assays in A and C, low avidity cells were substituted with and equivalent volume culture medium. Forty μl cell-free supernatant was harvested and percent specific release (PSR) of 51- Chromium calculated. Calculation of percent specific release was described previously (6). Percent inhibition was calculated by the formula: $100 \times (\text{PSR(high avidity + mel526)} - \text{PSR}_{(\text{high + low avidity + mel526})})/ \text{PSR(high avidity + mel526)}$. Bars reflect standard deviation between assays in three separate experiments. **(E)** Changes in expression of apoptotic markers 7AAD and Annexin V on mel526 target cells at 4 and 24 hours. Bar graph illustrates the percent change in apoptotic markers for each group (4 hour time point; High vs. Low; $p \leq 0.01$, High vs. Low + High; $p \leq 0.016$) and (24 hour time point; High vs. Low; $p \leq 0.01$, High vs. Low + High; $p \leq 0.01$). Assays were performed in triplicate.

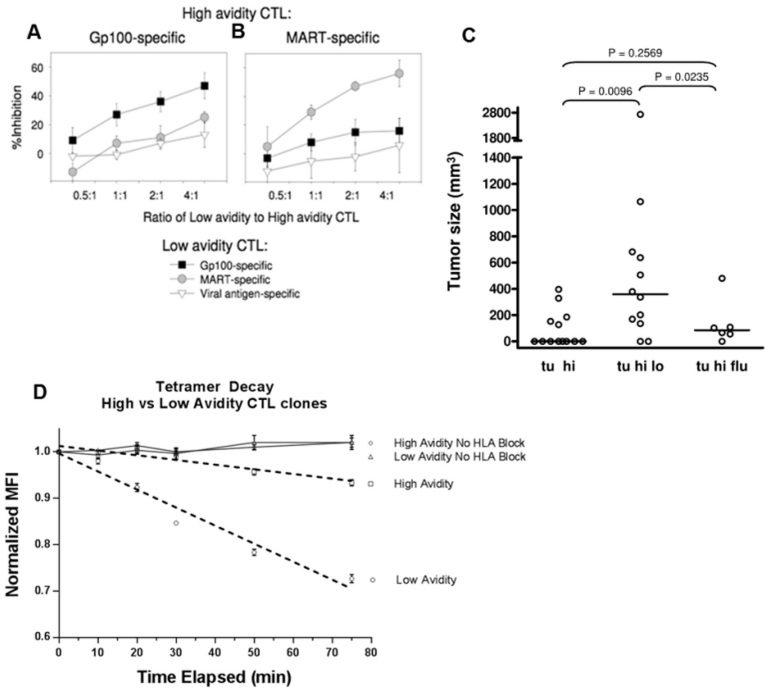

Figure 2. High avidity CTL lysis of tumor cells *in vitro* and suppression of tumor growth *in vivo* is inhibited by low avidity CTLs in an antigen-specific manner

Assays were performed as described in legend for Figure 1. Gp100-specific (**A**) or MART-specific (**B**) high avidity CTL were combined with Gp100-specific or MART-specific low avidity CTL, or FLU-specific CTL. Percent inhibition of melanoma cell lysis was calculated as in legend for Fig 1. Bars represent standard deviation between 3 separate assays, each performed in triplicate. (**C**) Suppression of tumor growth *in vivo* by high avidity CTLs was inhibited by low avidity CTLs, but not by a CTL clone of irrelevant specificity (flu peptide specific CTL). C57BL SCID (common gamma/RAG2 double knockout) mice were injected subcutaneously with mel526 human tumor cells. Results indicate tumor size 40 days post injection of G209n-specific high avidity CTL (tu hi), G209n-specific high avidity CTL combined with G209n-specific low avidity CTL (tu hi lo), or G209n-specific high avidity CTL combined with flu-specific CTL (tu hi flu). (**D**) Reduction of MFI of iTAg G209 specific MHC Class I Human Tetramer-SA-PE (normalized to initial MFI at 0 minutes) from CD8 labeled low (○) and high (□) avidity G209 specific CTL clones were plotted versus time elapsed post incubation with blocking HLA-A2 fab fragment. Also provided are control plots of low (Δ) and high (◇) avidity CTL clones that are tetramer/CD8 stained and collected at same time points without addition of HLA-A2 fab fragment. Results are representative of three separate experiments. Data were fitted using a linear mixed effects model to test intercept and slope over time by group effects. Calculations were based on the nlme package in R version 2.12.1.

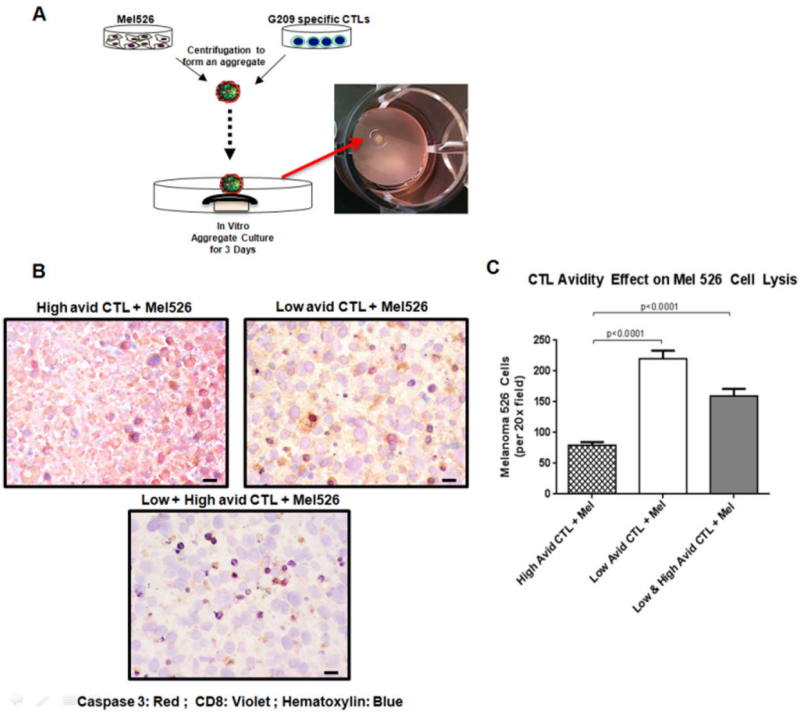

Figure 3. Visualizing CTL cross-inhibition in three dimensional (3D) culture system

(**A**) Schematic of generating mel526/CTL aggregates for in vitro models. Cultured mel526 cells (2×10^5 cells) plus either high (1×10^5) or low (1×10^5) avidity CTLs or combination of high and low avidity CTLs cells were mixed to form aggregates. Aggregates were then cultured on nucleopore membranes floating in DMEM medium supplemented with 10% FBS for 48 hours for in vitro analyses. (**B**) Paraffin embedded aggregate tissue sections from each group were analyzed for expression of melanin A (brown), haematoxylin (blue), and caspase 3 (red). Shown are representative sections. See “Materials and methods, Histologic analyses” for image acquisition information. (**C**) Bar graph representing the viable cell count of tumor aggregates. Counts were determined from the paraffin embedded sections of each aggregate imaged at 20x. Mean cell counts for 6 independent areas of each aggregate are reported. Unpaired t-test of the data groups was performed and statistical significance was given for $p<0.05$.

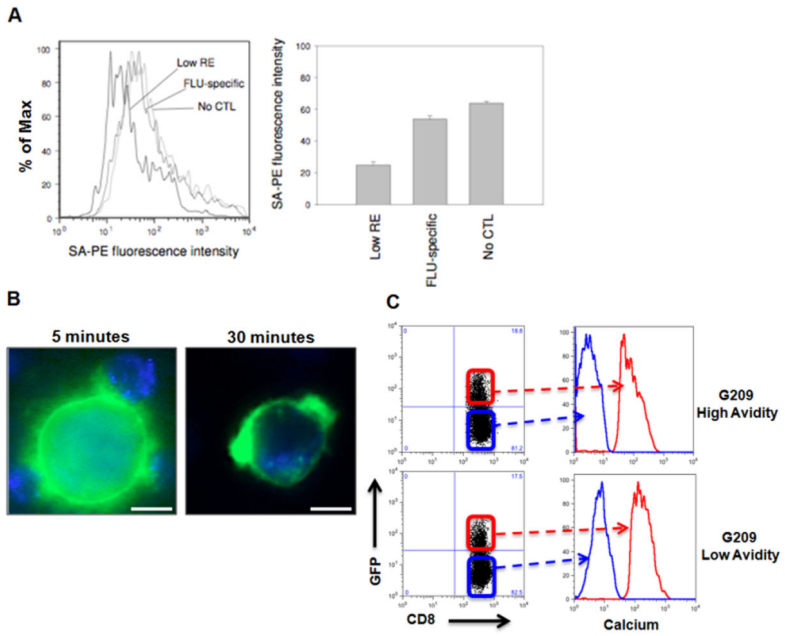

Figure 4. Low avidity CTLs reduce specific peptide-MHC complexes on the surface of tumor cells

(**A**) Changes in biotin-tagged cognate peptide levels analyzed for stripping from the surface of target cells by low avidity CTL. Remaining cognate peptide concentration analyzed by flow cytometry for streptavidin (SA)-PE fluorescence intensity. (**B**) To visualize trogocytosis, immortalized B-cells expressing HLA-A*02:01 coupled to GFP (HmyA2GFP cells) were pulsed with G209n-specific peptide and incubated with G209n-specific low avidity CTLs. Formation of clusters between CTLs and HmyA2GFP cells were visualized via live cell fluorescent microscopy at 5 min (left panel). Small membrane fragments of HLA-GFP expression on the surface of CD8+ T cells appeared after 15 to 30 minutes (right panel). (**C**) An increase in intracellular calcium concentration is directly associated with both high and low avidity CTLs undergoing trogocytosis. HmyA2GFP cells were pulsed with G209n peptide (1ng/ml) and incubated with either G209n high or low avidity CTLs for 7 minutes. Following incubation, GFP+CD8+ cells were gated and compared to GFP-CD8+ cells for the levels of intracellular calcium concentration.

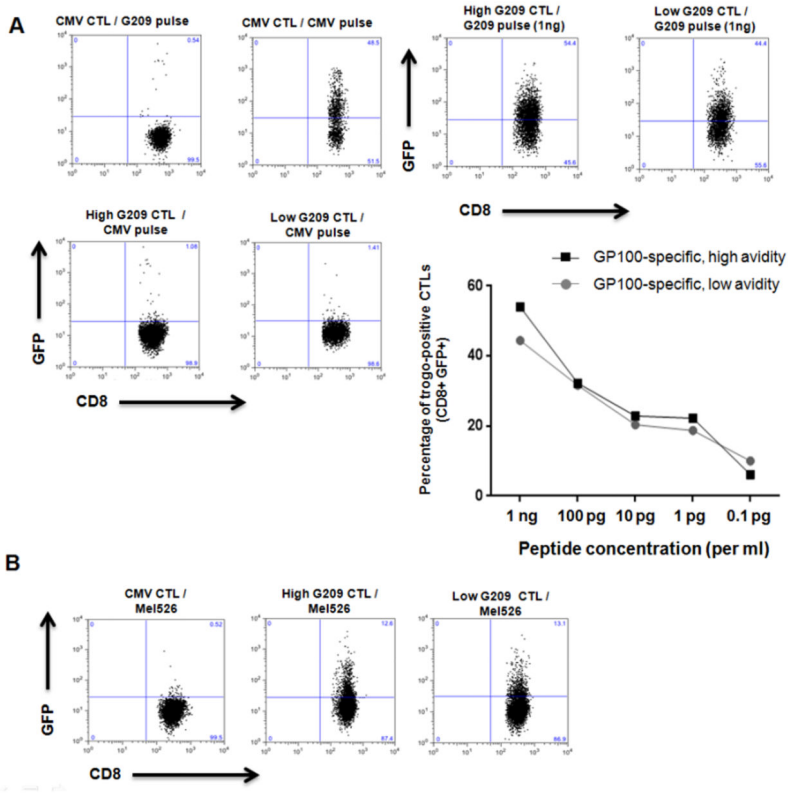

Figure 5. Level of trogocytosis is dependent on antigen specificity and peptide concentration and is equal in low and high avidity CTL clones

(**A**) FACS analysis showing the percent of trogocytosis of both high and low avidity CTL clones specific for G209n at 1ng/ml. Line graph shows increasing concentrations of G209n peptide on APCs show greater levels of trogocytosis for either CTL group. FACS analysis showing the levels of trogocytosis when incubating G209n specific high and low avidity CTLs with PKH67 labeled mel526 melanoma cells. (**B**) We used CMV specific CTLs as a control for measuring G209 specific trogocytosis in both pulsed HmyA2GFP and Mel526 cell line. The figure highlights peptide specificity of trogocytosis and the inability of CMV specific CTLs to undergo trogocytosis when incubated with Mel526 cell line.

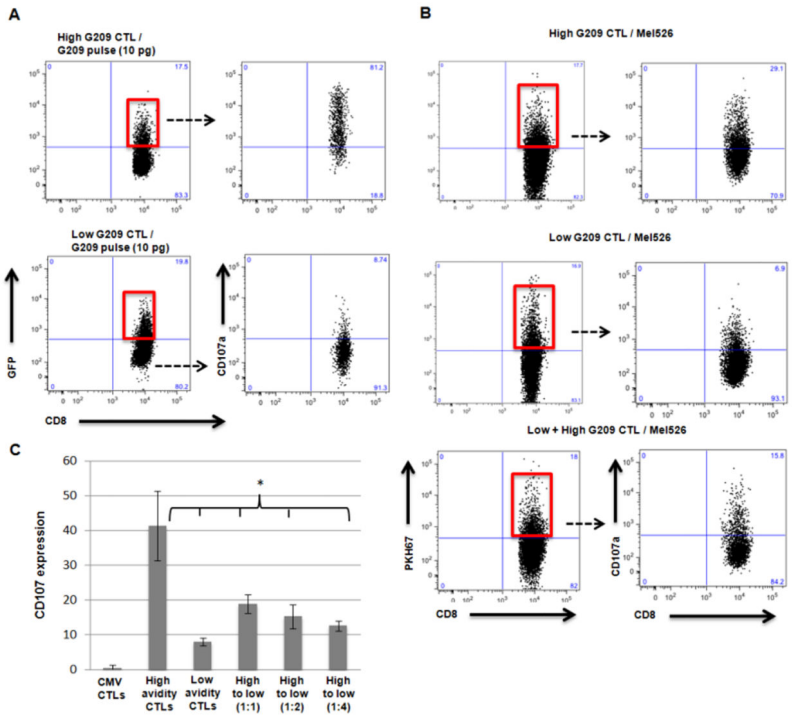

Figure 6. Suppression of degranulation by low avidity CTL

(**A**) FACS analysis showing expression of CD107A on trogocytosis positive populations of both low avidity CTLs and high avidity CTLs following incubation with G209n peptide pulsed HmyA2GFP cells. (**B**) FACS analysis showing differences in CD107A expression in trogocytosis positive populations of high avidity CTLs, low avidity CTLs, and impact of low avidity CTLs followed by addition of high avidity CTLs, when incubated with mel526 cell line labeled with PKH67. To measure the expression of CD107A on high avidity CTLs following incubation with low avidity CTLs, each CTL populations were separately stained with differently conjugated CD8 antibody (Pacific Blue for high avidity and Ds Red for low avidity) and gated on only Pacific Blue positive high avidity CTLs. (**C**) Overall percentage of CD107 expression selectively in high avidity effectors mixed with that of low avidity CTL clones (High vs. Low; $p \leq 0.028$, High vs. High + Low [1:1]; $p \leq 0.05$, High vs. High + Low [1:2]; $p \leq 0.035$, High vs. High + Low [1:4]; $p \leq 0.034$). Assays were performed in triplicate.

Table 1

Characterization of MART-1 and gp100-specific CTL clones by functional avidity

TAA specificity	Clone	[1] Avidity for native peptide	[2] Functional avidity
Gp100	476.139	11.2	High
	422.50	10.4	Intermediate
	422.47	10.0	Low (#1)
	476.105	8.3	Low (#2)
MART-1	461.9	8.2	High
	461.24	7.7	High
	520.31	5.1	Low
	517.7	5.1	Low
	461.10	6.1	Low
	517.2	6.4	Intermediate
	517.3	4.8	Low
	520.33	6.3	Intermediate

[1] Avidity for native peptide was determined as peptide concentration resulting in 40% lysis (~50% of maximum) of peptide-pulsed T2 cells. The generally higher values of gp100 compared to MART avidity scores is likely due to differences in peptide-MHC half-life between the two peptides.

[2] Functional avidity was determined by efficiency at melanoma cell lysis. Low: < 10% lysis. Intermediate: ≥ 10% to 40% lysis. High: > 40% lysis.